

01 Sep 1999

GalNAs Resonant-Cavity-Enhanced Photodetector Operating at 1.3 μm

J. B. Heroux

Xiaodong Yang

Missouri University of Science and Technology, yangxia@mst.edu

W. I. Wang

Follow this and additional works at: https://scholarsmine.mst.edu/mec_aereng_facwork



Part of the [Mechanical Engineering Commons](#)

Recommended Citation

J. B. Heroux et al., "GalNAs Resonant-Cavity-Enhanced Photodetector Operating at 1.3 μm ," *Applied Physics Letters*, vol. 75, no. 18, pp. 2716-2718, American Institute of Physics (AIP), Sep 1999.

The definitive version is available at <https://doi.org/10.1063/1.125126>

This Article - Journal is brought to you for free and open access by Scholars' Mine. It has been accepted for inclusion in Mechanical and Aerospace Engineering Faculty Research & Creative Works by an authorized administrator of Scholars' Mine. This work is protected by U. S. Copyright Law. Unauthorized use including reproduction for redistribution requires the permission of the copyright holder. For more information, please contact scholarsmine@mst.edu.

GaInNAs resonant-cavity-enhanced photodetector operating at 1.3 μm

J. B. Héroux,^{a)} X. Yang, and W. I. Wang

Department of Electrical Engineering, Columbia University, New York, New York 10027

(Received 19 July 1999; accepted for publication 8 September 1999)

We demonstrate a GaAs-based *p-i-n* resonant-cavity-enhanced (RCE) GaInNAs photodetector operating near 1.3 μm . The device design was optimized using a transfer matrix method and experimental absorption spectra obtained from *p-i-n* structures grown without a resonant cavity. The RCE photodetector was fabricated in a single growth step by using GaAs/AlAs distributed Bragg reflectors for the top and bottom mirrors. A 72% quantum efficiency was obtained with a full width at half maximum of 11 nm. © 1999 American Institute of Physics.
[S0003-6951(99)02444-4]

Resonant cavity enhanced (RCE) photodetectors have attracted much attention in the past few years due to their potential for high quantum efficiency, high speed, and narrow spectral bandwidth detection.¹ For *p-i-n* heterojunction photodiodes, the use of a Fabry–Perot cavity with optimized top and bottom reflectors makes it possible to reach a high quantum efficiency even if the normalized absorption coefficient αd of the intrinsic region is small, so that high speed operation is not limited by carrier drift time across the depletion region. However, in order to obtain a high quantum efficiency with a small normalized absorption coefficient, it is essential to use a bottom distributed Bragg reflector (DBR) with a near unity reflectance.²

The fabrication of a high speed, high quantum efficiency *p-i-n* RCE photodetector operating at 1.3 μm is especially important because of the low loss and low dispersion coefficients exhibited by optical fibers at this wavelength. However, with materials grown on InP substrates, it is difficult to get a DBR with a high reflectance because of the lack of a material system with a high refractive index difference between its layers. On GaAs substrates, GaAs and AlAs have a refractive index step of more than 14%, a value more than twice as large as that which can be obtained with InP-based materials.³ The use of a GaAs substrate to fabricate a photodetector is also more attractive because of a more advanced device technology; however the lattice mismatch between GaAs and $\text{In}_x\text{Ga}_{1-x}\text{As}$ used as an absorbing layer in the *p-i-n* structure increases rapidly with indium content so that device performance is seriously degraded for an operating wavelength greater than 1 μm . To circumvent this problem, Tan *et al.*^{3,4} used a wafer fusing technique to bond a *p-i-n* photodiode grown on InP with a GaAs/AlAs DBR grown on GaAs. By depositing a Si/SiO₂ top mirror after etching the InP substrate, a quantum efficiency higher than 90% was obtained at 1.3 μm . However, the fabrication requires two growth steps and the wafer fusing and etching processes are relatively complex. Campbell *et al.*⁵ demonstrated a GaAs-based narrow spectral bandwidth InGaAs quantum dot RCE photodiode operating at a wavelength close to 1.3 μm . A quantum efficiency of 49% was obtained, but the estimated

normalized absorption coefficient αd was very small, less than 0.01.

The $\text{Ga}_{1-x}\text{In}_x\text{N}_y\text{As}_{1-y}$ alloy is a material that may offer alternatives for conventional, single growth step RCE devices. The addition of a small amount of nitrogen to $\text{In}_x\text{Ga}_{1-x}\text{As}$ reduces both the band gap and the lattice mismatch with GaAs.⁶ As a result, the $\text{Ga}_{1-x}\text{In}_x\text{N}_y\text{As}_{1-y}$ compound is suitable for long wavelength (1.3–1.5 μm), GaAs-based optoelectronic devices. Recently, vertical cavity surface emitting lasers emitting at 1.285 μm (Ref. 7) and solar cells operating in the 1–1.2 μm range⁸ were demonstrated with this material.

In this letter, we report on the growth and characterization of a GaInNAs RCE photodetector. The device combines the advantages of a high reflectance, large spectral bandwidth GaAs/AlAs bottom DBR and a small band-gap GaInNAs absorbing region. Transfer matrix method simulations using experimental absorption coefficients obtained from *p-i-n* structures grown without a resonant cavity were done in order to adjust material parameters for a high quantum efficiency at 1.3 μm . An experimental peak external quantum efficiency of 72% was obtained.

The samples were grown by molecular beam epitaxy using a Varian Gen-II system equipped with a rf nitrogen source (Oxford Applied Research Model MDP 21). Growth conditions were optimized in order to get a good material quality and a high nitrogen concentration in the material.⁹ An antimonide flux of 1.8×10^7 Torr was present during growth of the GaInNAs layers. The nitrogen concentration was estimated to be 1% by x-ray diffraction, absorption, and secondary ion mass spectroscopy.¹⁰

We adopted a structure with multiple absorbing regions¹¹ (Fig. 1) designed to provide a high quantum efficiency with a small normalized absorption coefficient αd so that a smaller fraction of indium had to be incorporated in the absorbing layers and the lattice mismatch was reduced. First, an n^+ doped (Si: $2 \times 10^{18} \text{ cm}^{-3}$) 20 period GaAs/AlAs DBR was grown on an n^+ GaAs (100) substrate. The GaAs/ $\text{Ga}_{1-x}\text{In}_x\text{N}_{0.01}\text{As}_{0.99}$ *p-i-n* structure was grown on top of this DBR with its optical length adjusted for resonance at 1.3 μm . The three 400 Å thick absorbing layers were positioned at maxima of the optical field. Undoped GaAs spacer layers were used to prevent diffusion of the dopants in the

^{a)}Electronic mail: jbh14@columbia.edu

5X	GaAs	p+	953 Å
	AlAs	p+	1115 Å
	GaAs	p+	1547 Å
	GaAs	i	100 Å
	GaInNAs:Sb	i	400 Å
	GaAs	i	1424 Å
	GaInNAs:Sb	i	400 Å
	GaAs	i	1424 Å
	GaInNAs:Sb	i	400 Å
	GaAs	i	100 Å
20X	GaAs	n+	595 Å
	GaAs	n+	953 Å
	AlAs	n+	1115 Å
	GaAs buffer	n+	5000 Å
	GaAs subs	n+	

FIG. 1. Schematic diagram of the layer profile of a RCE *p-i-n* photodetector with multiple absorbing regions. The GaInNAs layers are positioned at maxima of the optical field.

absorbing layers. A p^+ doped (Be: $2 \times 10^{18} \text{ cm}^{-3}$) GaAs/AlAs DBR was grown on the *p-i-n* structure to get an optimal top reflectance given by $R_{\text{top}} = R_{\text{bot}} \exp(-2\alpha_{\text{eff}}d)$ where R_{top} (R_{bot}) is the top (bottom) mirror reflectance and $\alpha_{\text{eff}}d \approx 2ad$ is the effective normalized absorption coefficient which takes into account the standing wave effect.²

Mesas with diameters ranging from 300 μm to 1 mm were etched down to the buffer layer. Gold layers were evaporated on top of the mesas and on the buffer layer in a single liftoff step to form ohmic contacts. Photocurrent measurements were taken using a Bomem DA8 Fourier transform infrared spectrometer (FTIR), a current preamplifier, and a dc bias voltage source. The quantum efficiency of the samples was calculated by comparing photocurrent spectra from 1 mm diameter mesas to the spectra of a germanium photodiode with the same active diameter for which the responsivity was known (Germanium Power Devices Inc.). Quasinormal incidence reflectance measurements were also obtained with the FTIR using a gold mirror as a reference.

Conventional *p-i-n* structures similar to the one shown in Fig. 1 but without the DBR regions were grown to determine the absorption coefficient of the $\text{Ga}_{1-x}\text{In}_x\text{N}_{0.01}\text{As}_{0.99}$ layers. The reflectance and the quantum efficiency for samples with $x=0.20$ and 0.25 are presented in Fig. 2. The normalized absorption coefficient ad , also shown in Fig. 2, was calculated from these experimental values using well-known relations.¹² Assuming a complete photogenerated carrier collection efficiency, we estimate that the lower boundary values for ad at 1.3 μm are 0.027 for $x=0.20$ and 0.06 for $x=0.25$.

Figure 3 shows a transfer matrix method simulation of the peak quantum efficiency at 1.3 μm as a function of the bottom DBR reflectance for a RCE *p-i-n* photodetector using the experimental absorption coefficients of Fig. 2. The number of periods of the top DBR N_{top} used for the simulations was 7 and 5 for indium concentrations of 20% and 25%, respectively, corresponding to nearly optimal reflectances R_{top} of 88% and 78%. To simulate a lowering of the bottom

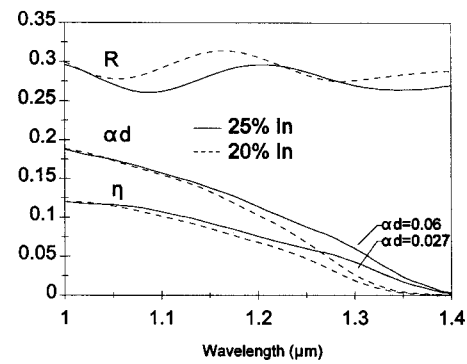


FIG. 2. Experimental reflectance (R), quantum efficiency (η), and normalized absorption coefficient (ad) spectra of conventional *p-i-n* structures (i.e., without a resonant cavity) similar to the one illustrated in Fig. 1 with indium concentrations of 20% and 25% in the absorbing layers.

reflectance due to possible experimental imperfections, the number of periods of the bottom DBR was varied from 20 to 14, the two rightmost data points corresponding to the ideal case of a 20 period DBR with a reflectance $R_{\text{bot}} = 99.3\%$. The calculated full width at half maximum (FWHM) was 6 and 11 nm, respectively, for indium fractions $x=0.20$ and $x=0.25$. Figure 3 shows that even though a quantum efficiency higher than 90% should in principle be obtained with a 20 period bottom DBR for both indium concentrations, the higher concentration case is much less sensitive to a possibly slightly lower than expected experimental reflectance of the bottom DBR. Consequently, we chose to demonstrate experimentally this latter case.

Figure 4 shows the experimental spectra of the reflectance and quantum efficiency obtained for a RCE photodetector with 25% indium in the absorbing regions. The optical thickness of the resonant cavity was calibrated by first growing a *p-i-n* structure on top of a five-period DBR providing a reflectance high enough to clearly observe a dip due to resonant absorption. As shown in Fig. 4, a peak quantum efficiency of 72% and a FWHM of 11 nm were obtained at a wavelength of 1.292 μm with a reverse bias of 7 V. The resonant wavelength was very close to 1.3 μm and the FWHM was in very good agreement with the simulated results of Fig. 3. The reflectance drop to 5% at resonance was also within a few percent of the theoretical value found by transfer matrix method. The 25% difference between the ex-

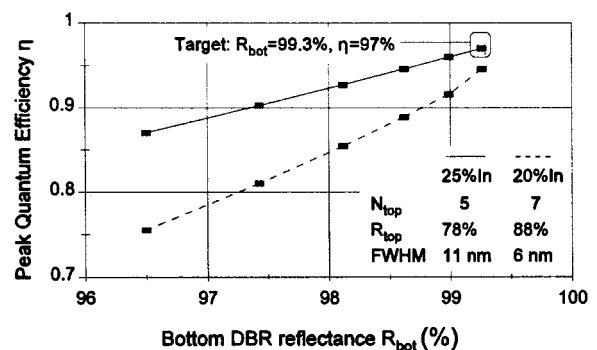


FIG. 3. Simulated peak quantum efficiency η at 1.3 μm of a RCE *p-i-n* photodetector as a function of the bottom DBR reflectance using the experimental absorption values of Fig. 2. N_{top} , R_{top} , and R_{bot} are the number of periods of the top DBR and reflectance of the top bottom DBR, respectively. FWHM is the full width at half maximum of the peak quantum efficiency.

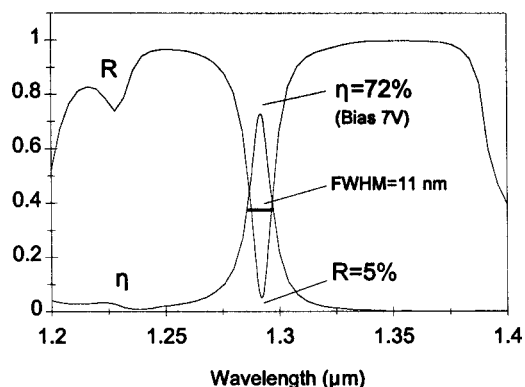


FIG. 4. Experimental reflectance and quantum efficiency spectra of a RCE *p-i-n* photodetector.

perimental and simulated peak quantum efficiency is likely due to carrier trapping at the GaInNAs/GaAs interfaces or to recombination centers caused by defects in the material. A lower than expected quantum efficiency has also been observed by Murtaza *et al.*¹³ for similar structures grown using conventional, lattice-matched material systems so that it is probably not due to a low material quality in our case. A simple saturation of the responsivity caused by the resonant cavity has to be ruled out since our results were not improved by decreasing the incoming light power.

The leakage current of the photodetector was 0.7, 2.0, and 7.5 μA for a 1 mm mesa at biases of 3, 5, and 7 V with peak quantum efficiencies of 48%, 63%, and 72%, respectively. This high leakage current may be reduced. Further growth optimization to incorporate more nitrogen and reduce the lattice mismatch is possibly a solution even though this has proven to be difficult and may degrade the material quality (see, for example, Ref. 9). Sample annealing has not yet

been investigated and may also improve performance (see, for example, Ref. 8) provided it has a negligible effect on the reflectance of the bottom DBR and on the doping profile. Using strain-compensated multiple quantum wells¹⁴ as an absorbing region may also be a promising alternative.

In conclusion, we have demonstrated a GaInNAs RCE photodetector grown on GaAs operating at 1.3 μm . A 72% quantum efficiency was obtained with a FWHM of 11 nm. The GaAs/GaInNAs material system is promising for long wavelength (1.3–1.55 μm) RCE devices such as photodetectors, modulators, and phototransistors.

¹M. S. Unlu and S. Strite, *J. Appl. Phys.* **78**, 607 (1995).

²K. Kishino, M. S. Unlu, J. I. Chyi, J. Reed, L. Arsenault, and H. Morko , *IEEE J. Quantum Electron.* **27**, 2025 (1991).

³I.-H. Tan, E. L. Hu, J. E. Bowers, and B. I. Miller, *IEEE J. Quantum Electron.* **21**, 1863 (1995).

⁴I.-H. Tan, J. J. Dudley, D. I. Babic, D. A. Cohen, B. D. Young, E. L. Hu, J. E. Bowers, B. I. Miller, U. Koren, and M. G. Young, *IEEE Photonics Technol. Lett.* **6**, 811 (1994).

⁵J. C. Campbell, D. L. Huffaker, H. Deng, and D. G. Deppe, *Electron. Lett.* **33**, 1337 (1997).

⁶M. Kondow, K. Uomi, A. Niwa, T. Kitatani, S. Watahiki, and Y. Yazawa, *Jpn. J. Appl. Phys., Part 1* **35**, 1273 (1996).

⁷C. Ellmers, F. Hohnsdorf, J. Koch, C. Agert, S. Leu, D. Karaiskaj, M. Hofmann, W. Stolz, and W. W. Ruhle, *Appl. Phys. Lett.* **74**, 2271 (1999).

⁸S. R. Kurtz, A. A. Allerman, E. D. Jones, J. M. Gee, J. J. Banas, and B. E. Hammons, *Appl. Phys. Lett.* **74**, 729 (1999).

⁹X. Yang, J. B. H eroux, M. J. Jurkovic, and W. I. Wang, *J. Vac. Sci. Technol. B* **17**, 1144 (1999).

¹⁰X. Yang, M. J. Jurkovic, J. B. H eroux, and W. I. Wang, *Appl. Phys. Lett.* **75**, 178 (1999).

¹¹F. Y. Huang, A. Salvador, X. Gui, N. Teraguchi, and H. Morko , *Appl. Phys. Lett.* **63**, 141 (1993).

¹²S. M. Sze, *Physics of Semiconductor Devices* (Wiley, New York, 1981).

¹³S. S. Murtaza, R. V. Chelakara, R. D. Dupuis, and J. C. Campbell, *Appl. Phys. Lett.* **69**, 2462 (1996).

¹⁴T. Miyamoto, S. Sato, Z. Pan, D. Schlenker, F. Koyama, and K. Iga, *J. Cryst. Growth* **195**, 421 (1998).